Journal of Applied Polymer Science

ZIF-11/Polybenzimidazole Composite Membrane with Improved Hydrogen Separation Performance

Lunxi Li,[1] Jianfeng Yao,[1] Xiaojing Wang,[2] Yi-Bing Cheng,[2] Huanting Wang[1]

[1]Department of Chemical Engineering, Monash University, Clayton, Victoria 3800, Australia

[2]Department of Materials Engineering, Monash University, Clayton, Victoria 3800, Australia

Correspondence to: J. Yao (E-mail: jianfeng.yao@monash.edu) and H. Wang (E-mail: huanting.wang@monash.edu)

ABSTRACT: Zeolitic imidazolate framework (ZIF)-11 crystals were prepared by the toluene-assisted method, and they were incorporated into polysulfone, polyethersulfone, and polybenzimidazole (PBI) matrix to investigate the compatibility. ZIF-11 had a good connection with PBI matrix as they had the same benzimidazole groups. The evaporation temperature of the membrane formation was studied with two different solvents: *N*-methyl-2-pyrrolidone (NMP) and *N*,*N*-dimethylacetamide (DMAc). Then, the ZIF-11/PBI composite membranes prepared using NMP or DMAc as the solvent were characterized and tested by gas separation. Improved H_2 and CO_2 permeabilities with a H_2/CO_2 ideal selectivity of 5.6 were obtained on the 16.1 wt % ZIF-11/PBI composite membrane prepared with DMAc as the solvent. © 2014 Wiley Periodicals, Inc. J. Appl. Polym. Sci. **2014**, *131*, 41056.

KEYWORDS: compatibilization; composites; membranes

Received 30 April 2014; accepted 22 May 2014

DOI: 10.1002/app.41056

INTRODUCTION

Gas separation using membranes has been extensively studied because it is considered to be one of the most energy-efficient separation processes. Among candidate materials for membrane fabrication, polymers remain the most practical and economical choice.[1] The gas permeation through polymeric membranes is generally controlled by the solution-diffusion model.[2] However, the polymer membranes suffer from a trade-off between permeability and selectivity, that is, polymers with high selectivity present low permeability and *vice versa*. Such a trade-off behavior can be captured via an empirical upper-bound relationship as summarized by Robeson.[3] Mixed matrix membranes (MMMs) are based on solid–solid system composed of inorganic-dispersed phase inserted in a polymer matrix.[4] These kinds of membranes have the potential to achieve higher selectivity and permeability and beyond the upper-bound trade-off line.[5,6] However, one of the most critical issues is the incompatibility between the filler and the polymeric phase, resulting in a decrease in the selectivity. Nanosized fillers are expected to partially solve the incompatibility issue between fillers and the polymers and to increase the separation performance.[4,7,8]

Metal organic frameworks (MOFs) are a group of crystalline materials that have nanoporous networks composed of transition metal complexes and organic linkers. Typically, MOFs show high porosity with tailorable cavity sizes. As a subfamily of MOFs, zeolitic imidazolate frameworks (ZIFs) not only exhibit the advantages of MOFs but also have exceptional high thermal and chemical stability.[9,10] Studies on ZIF membranes with supports have shown promising gas separation properties for various gas pairs.[4,11,12] However, to prepare defect-free ZIF membranes with good mechanical strength and low cost remains a big challenge for research before they can be used for practical applications. One possible way is to incorporate ZIF particles into a polymer matrix membrane. Furthermore, because of the organic linkers presented in ZIF structure, it is believed that ZIFs can achieve better affinity and interaction with polymeric materials. Polybenzimidazole (PBI) is a promising polymeric membrane material because of its outstanding physical, thermal, and chemical stability.[13,14] In additional, PBI membrane could be easily fabricated because it is soluble in solvents such as *N*-methyl-2-pyrrolidone (NMP) and *N*,*N*-dimethylacetamide (DMAc). According to the literature, some research groups have investigated PBI MMM for gas separation.[8,15–17] By mixing the as-synthesized ZIF-7 nanoparticles without the traditional drying process with PBI, the resultant membranes not only achieved an unprecedented ZIF-7 loading as high as 50 wt % but also overcame the low permeability nature of PBI. Mixed gas separation was conducted from ambient temperature to 180°C and showed a significant increase in H_2 permeability but without compromising H_2/CO_2 selectivity.[15] Similarly, ZIF-8 and ZIF-90 nanocrystals have also been incorporated into PBI with high loadings, and the composite membranes exhibited enhanced H_2 permeability.[8,16,17] For example, the 30% ZIF-8/PBI composite membrane enhanced the H_2

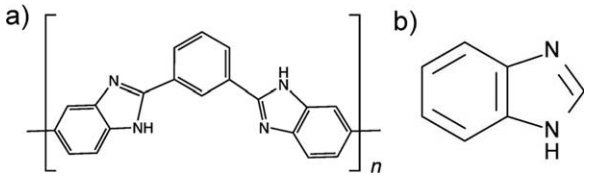

Figure 1. Chemical structures of polybenzimidazole (a) and the benzimidazole group in ZIF-11 (b).

permeability from 3.7 to 105.4 Barrer together with improved H_2/CO_2 selectivity from 8.7 to 12.3 at 35°C, far surpassing the Robeson upper bound and other polymeric materials in the literature.[8] ZIFs incorporated in a large range of polymers for MMMs were summarized in our recent review.[4]

In this work, we incorporated ZIF-11 crystals into PBI polymeric membrane to increase the membrane performance. ZIF-11 with a RHO topology possesses large cages (14.6 Å) connected through small apertures (3.0 Å). The small pore size in ZIF-11 can block larger gases, but can let the smaller gas such as hydrogen pass through. The molecular simulation revealed that ZIF-11 has the potential to meet industrial requirements for H_2/CO_2 and H_2/N_2 separations.[18] However, as far as our knowledge, ZIF-11 has not been used as membrane material probably because (1) ZIF-11 materials only can be synthesized under critical conditions, and the particle size is usually over several micrometer; and (2) for ZIF-11 membrane formation, it is hard to grow a continuous layer. Recently, we developed a facile method to prepare ZIF-11 under the assistance of toluene at room temperature,[19] which will lead to the broader application of ZIF-11. Furthermore, as the benzimidazole group of ZIF-11 is the same as the unit group of PBI (Figure 1), the compatibility between ZIF-11 and PBI matrix should be good. ZIF-11/PBI composite membrane is expected to show improved H_2 separation performance.

EXPERIMENTAL

Chemicals

PBI {poly[2,2′-(*m*-phenylene)-5,5′-bibenzimidazole], 26 wt % of PBI, 1.5 wt % of LiCl in DMAc solvent} was purchased from PBI Performance Products and used as received. LiCl was originally added in the commercial PBI as a stabilizer to prevent aggregation of PBI molecules in the DMAc solution. NMP, DMAc, polysulfone (PS), polyestersulfone (PES), zinc acetate dihydrate [$Zn(CH_3COO)_2{\cdot}2H_2O$, 98%], benzimidazole ($C_7H_6N_2$, 98%), toluene, ammonium hydroxide solution (HN_3, 28–30% aqueous solution), and methanol (for analysis) were all purchased from Sigma-Aldrich, Australia. All the reagents and solvents were used as received without further purification.

Synthesis of ZIF-11 Crystals

ZIF-11 crystals were synthesized at room temperature according to our recent work.[19] In a typical synthesis, 0.12 g of benzimidazole was first dissolved in 8 g of methanol; the solution was stirred until the benzimidazole was totally dissolved. 2 g of toluene was added to the above solution, and the solution was stirred for 5 min. Then, 0.07 g of ammonium hydroxide solution was dropped into the solution under stirring for another 5 min. Finally, 0.11 g of zinc acetate dihydrate was added to the above solution with a continuous stirring for 4 h at room temperature. After the reaction, the product was collected by centrifugation, washed with methanol several times, and then dried at 120°C overnight to evaporate the trapped toluene and methanol.

ZIF-11 Dispersed in Different Polymers

To investigate the compatibility of ZIF-11 particles in different polymers, ZIF-11 crystals were mixed with PS, PES, and PBI separately by using NMP as the solvent. To obtain enough viscosity for further film casting, the weight percent of polymer in NMP solvent was fixed as 8.7 wt % for PBI solution (1.0 g PBI solution and 2 g of NMP), 16 wt % for PS solution (0.4 g of PS and 2 g of NMP), and 13 wt % for PES solution (0.3 g of PES and 2 g of NMP). A calculated amount of ZIF-11 (0.02 g in PS solution; 0.015 g in PES solution; and 0.05 g in PBI solution) was mixed with the above three solutions separately for film casting. Finally, the films were obtained by evaporating the solvent at 70°C overnight.

PBI Membrane Fabrication

PBI membranes were prepared using a typical knife-casting method. To investigate the membrane performance influenced by the evaporation temperature, pure PBI membrane was first prepared by dissolving 1 g of PBI solution in 2 g of NMP and DMAc separately. The solution was continuously stirred for 24 h, followed by casting the solution on a glass plate, and then the glass plate was put in an oven for solvent evaporation at three different temperatures (30–120°C) overnight. After cooling to room temperature, the formed membrane was peeled off from the glass plate, washed with water, and dried at 120°C overnight.

ZIF-11/PBI composite membranes were prepared as follows. First, a calculated amount of the as-synthesized ZIF-11 crystals (0.05, 0.11, and 0.17 g) was dispersed in 2.0 g of NMP or DMAc solvent, followed by sonication using an unltrasonicator (70 W, Branson, 1510E-DTH) for 1 h. Second, 1.0 g of PBI solution was added to the above solution, and the whole solution was stirred continuously for 24 h. Before membrane casting, the solution was ultrasonicated again for another 1 h to finely disperse the ZIF-11 crystals and to remove the trapped air bubbles. The casting solution was then poured onto a glass plate and casted by the casting knife with a designable air gap (200 μm). Subsequently, the glass plate was put in an oven for solvent evaporation at 70°C overnight. After cooling to room temperature, the formed membrane was peeled off from the glass plate. To ensure the full removal of the trapped solvent and LiCl, the resulting membranes were immersed in water overnight and then further dried at 120°C for 24 h.

The loading of ZIF-11 in the membrane is indicated as weight percentage and is defined by the following equation:

$$\text{Particle loading} = \frac{\text{Weight of particle}}{\text{Weight of particle} + \text{Weight of polymer}} \times 100\%.$$

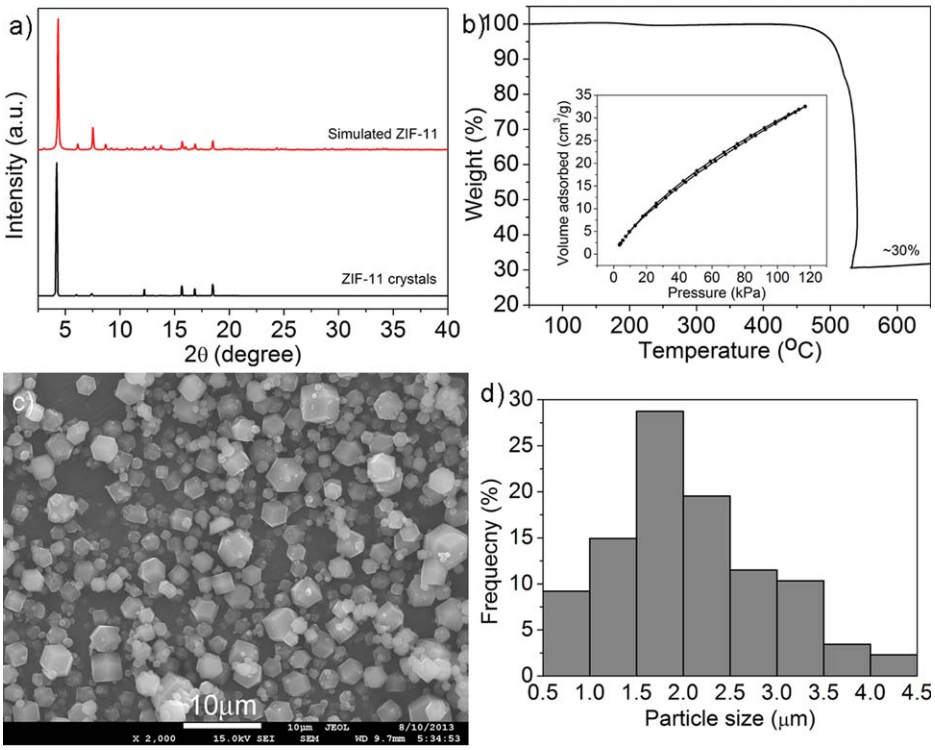

Figure 2. XRD patterns (a), TG curve (b), CO_2 adsorption–desorption isotherm (inset, b), SEM image (c), and the particle size distribution (d) of ZIF-11 crystals. [Color figure can be viewed in the online issue, which is available at wileyonlinelibrary.com.]

Characterization

Scanning electron microscopy (SEM) images of surfaces and cross-sections of membranes were taken with a JSM-7001F microscope (JEOL). The particle size distribution of ZIF-11 was determined by manual measurement of about 200 crystals in the SEM image. X-ray diffraction (XRD) patterns were recorded on a Philips PW 1140/90 diffractometer with Cu Kα radiation (25 mA and 40 kV) at a scan rate of 2°/min with a step size of 0.02°. Thermogravimetric analysis (TGA) was carried out with SII Exstar TG/DTA 6300 up to 650°C at a heating rate of 5°C/min. Carbon dioxide adsorption–desorption isotherm was measured using a volumetric adsorption analyzer (Micrometrics ASAP 2010) at ice water temperature of 273 K. The sample was degassed at 100°C under vacuum for 6 h prior to analysis. Fourier transform infrared (FTIR) spectra were recorded on a Perkin-Elmer FTIR spectrometer over a wavenumber range of 600–4000 cm^{-1}.

Single-Gas Separation Test

Gas separation was tested with the similar method described in Ref. 12. Briefly, to measure the gas permeation rate, the ZIF-11 composite membrane was attached to a porous stainless steel disk and sealed with Torr Seal epoxy resin (Varian) that the one side of the membrane was outward. Then, it was placed inside a large tube with a feed gas flowing through, and the permeate side was connected to a sensor and vacuum pump. For each single-gas measurement, the permeate side was vacuumed first, the permeate stream was then shut off from vacuum, and the pressure rise was recorded by the pressure sensor [Series 901 Transducer (MKS)]. All the gas permeation tests were performed at room temperature on pure H_2 and CO_2. Permeability of the PBI composite membrane was calculated by the following equation:

$$P_i = \frac{N_i l}{\Delta P_i A}, \quad (2)$$

where N_i is the permeation rate of component i (cm^3/s), l is the membrane thickness (cm), A is the membrane area (cm^2), and Δp_i is the pressure difference between two sides of the membrane (cmHg).

RESULTS AND DISCUSSION

Characterizations of ZIF-11 Particles

ZIF-11 crystals were synthesized by a facile method that was developed by our group.[19] ZIF-11 was first characterized via different methods. Figure 2(a) shows the XRD pattern of the dry ZIF-11 powder. The ZIF-11 crystals exhibit peaks that are well matched to the simulated ZIF-11 XRD pattern in the literature,[9] confirming the successful formation of ZIF-11 structure by this synthesis method. The TG curve shown in Figure 2(b) indicates that ZIF-11 is thermally stable up to 450°C in air. Although, the aperture size of ZIF-11 is smaller than the kinetic diameter of nitrogen, it is able to absorb carbon dioxide. The carbon dioxide adsorption–desorption curves [inset of Figure 2(b)] show that ZIF-11 has CO_2 uptake of 33 cm^3/g at 273 K. Figure 2(c) shows the SEM image of ZIF-11 particles with a rhombic dodecahedron structure. The average crystal size of ZIF-11 is about 2.0 μm with a size range of 0.5–4.5 μm [Figure 2(d)]. The particle size of ZIF-11 is controllable to some extent by

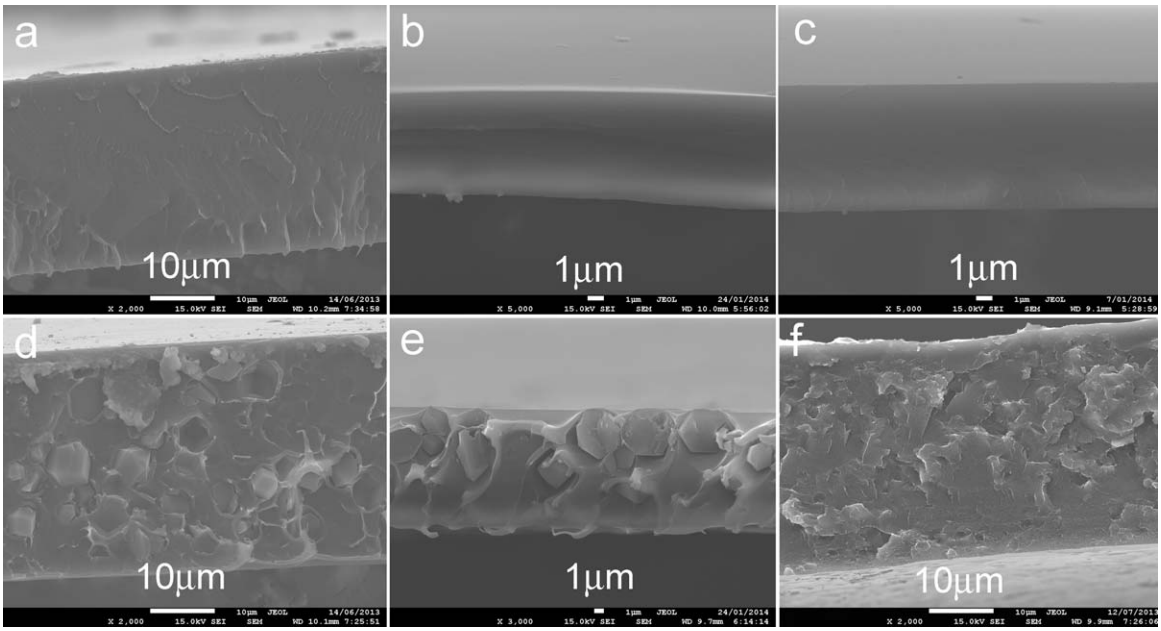

Figure 3. Cross-sectional SEM images of pure polymer membranes (a–c) and ZIF-11/polymer composite membranes (d–f): PS (a), PES (b), PBI (c), 4.7 wt % ZIF-11/PS (d), 4.7 wt % ZIF-11/PES (e), and 16.1 wt % ZIF-11/PBI (f).

varying the amount of ammonium hydroxide used in the synthesis solution.[19]

ZIF-11 Crystals in Different Polymers

Figure 3(a–c) shows cross-sectional SEM images of three pure PS, PES, and PBI films. Their morphologies are very similar. However, after incorporating ZIF-11 crystals, the morphologies become much different as shown in Figure 3(d–f). The boundary between ZIF-11 particles and PS [Figure 3(d)] can be easily observed, indicating that the compatibility between them is very poor, which causes the void formation at the interfacial region, resulting in a "sieve-in-a-cage" problem. A similar problem also happens in ZIF-11/PES film [Figure 3(e)], where ZIF-11 particles separate from the polymer matrix. The poor compatibility between ZIF-11 and polymer will directly lead to poor gas separation performance. However, ZIF-11 particles in PBI

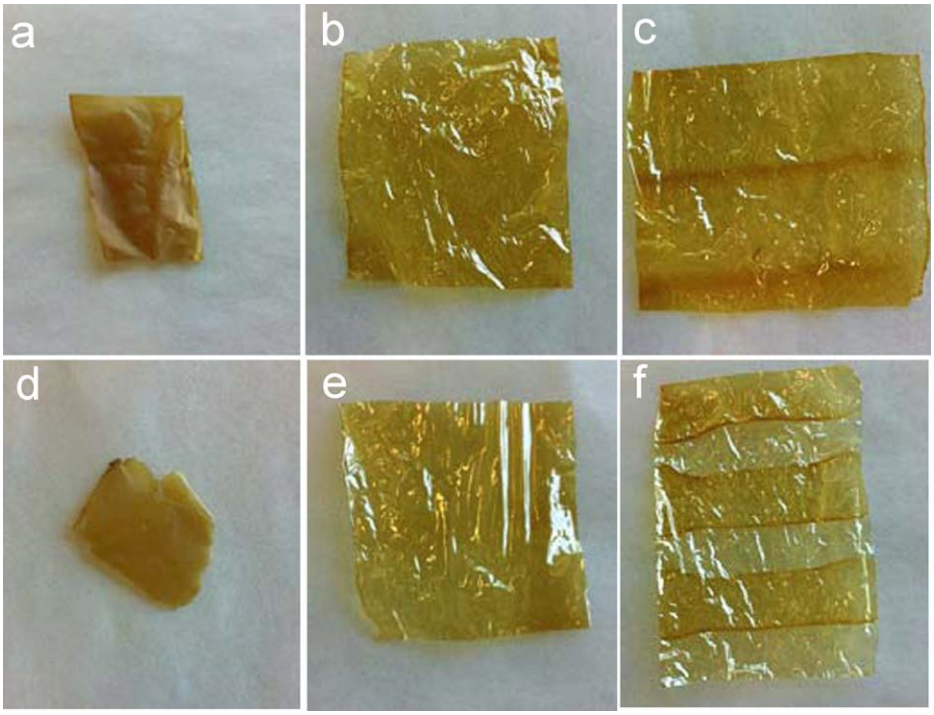

Figure 4. The digital photos of PBI membranes prepared with NMP (a–c) or DMAc (d–f) as the solvent and evaporated at 30°C (a and d), 70°C (b and e), and 120°C (c and f). [Color figure can be viewed in the online issue, which is available at wileyonlinelibrary.com.]

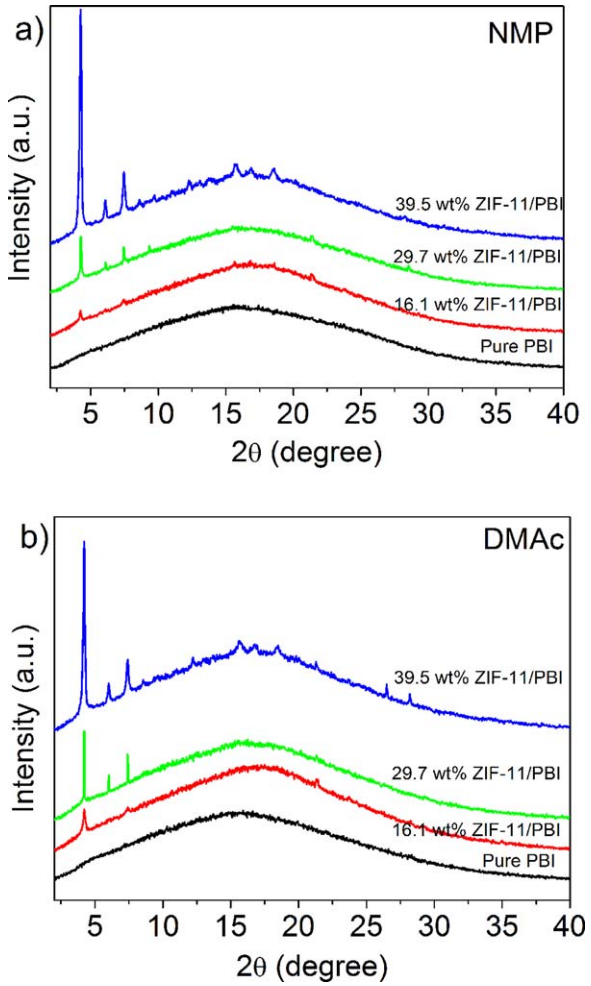

Figure 5. XRD patterns of ZIF-11/PBI membranes prepared with NMP (a) and DMAc (b) solvents. [Color figure can be viewed in the online issue, which is available at wileyonlinelibrary.com.]

present a good compatibility [Figure 3(f)]. There is no clear boundary between ZIF-11 and PBI, indicating that ZIF-11 crystals bond well with PBI matrix.

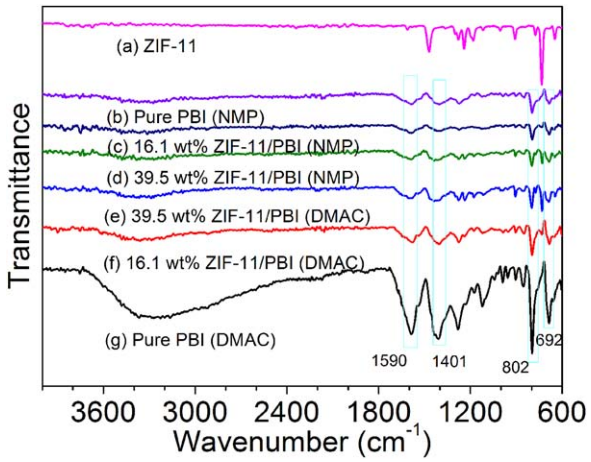

Figure 6. FTIR spectra of ZIF-11, pure PBI, and ZIF-11/PBI composite membranes. [Color figure can be viewed in the online issue, which is available at wileyonlinelibrary.com.]

Effect of Evaporation Temperature

The solvent evaporation rate is very crucial for the membrane quality. Pure PBI membrane was prepared at different evaporation temperatures (30, 70, and 120°C) using NMP or DMAc as the solvent. As shown in Figure 4, their appearances are quite different at different temperatures. However, for the two different solvents, the resulting membranes show similar morphologies at the same temperature because the evaporation temperature is less than the boiling point of the solvents (NMP: 202°C; DMAc: 165°C). For the membrane evaporated at 30°C, the color of membrane is dark and opaque. In addition, the membranes become thicker probably due to the absorption of atmospheric water that precipitates the polymer, producing a hazy surface. When the evaporation temperature is 120°C, the fabricated membranes are transparent, but not even, especially for the membrane prepared with DMAc solvent [Figure 4(f)]. A suitable evaporation rate is necessary to form a good performance membrane. The membranes fabricated at 70°C are very transparent with a good toughness and shows a uniform color and thickness.

ZIF-11/PBI Composite Membranes

XRD measurements between 2° and 40° were conducted to determine the crystalline structure of ZIF-11/PBI composite membranes. As shown in Figure 5, the XRD patterns of the membranes show ZIF-11 peaks matching well with the pure ZIF-11 structure, indicating that ZIF-11 crystalline structure remains unchanged after being incorporated into the PBI matrix with NMP or DMAc as the solvent. With the increase of ZIF-11 loadings from 16.1 to 39.5 wt % in the PBI matrix, the XRD intensities of ZIF-11 become stronger for both composite membranes using different solvents. TGA analysis of the ZIF-11/PBI composite membranes with NMP or DMAc as the solvent under nitrogen (not shown) indicates the complete removal of solvents as there is no weight loss before 400°C.

Figure 6 shows the FTIR spectra of ZIF-11 crystals, pure PBI, and ZIF-11/PBI composite membranes prepared with NMP or DMAc as the solvent. Figure 6 (Peak a) shows the typical characteristic spectrum of ZIF-11.[19] The peaks at 692, 802, 1401, and 1590 cm^{-1} are assigned to C—H out-of-plane bending of 3,4-disubstituted biphenyl, heterocyclic ring vibration or C—H out-of-plane bending of three adjacent hydrogen atoms in substituted benzene rings, C—C stretching, and ring vibration characteristics of conjugation between benzene and imidazole rings, respectively, and they are all the characteristic peaks of PBI.[20] For the composite membrane prepared with NMP as the solvent, the characteristic peaks at 692, 802, 1401, and 1590 cm^{-1} only have a little decrease after the addition of 16.1 or 39.5 wt % ZIF-11 (Figure 6, Peaks b–d). However, for the 16.1 or 39.5 wt % ZIF-11/PBI composite membrane with DMAc as the solvent, the peaks at 692, 802, 1401, and 1590 cm^{-1} have a significant decrease (Figure 6, Peaks e–g), indicating a strong interaction between ZIF-11 and PBI.

SEM analysis was carried out to investigate the morphology of the ZIF-11/PBI composite membranes and the compatibility between ZIF-11 and PBI. Figure 7 shows the SEM images of the

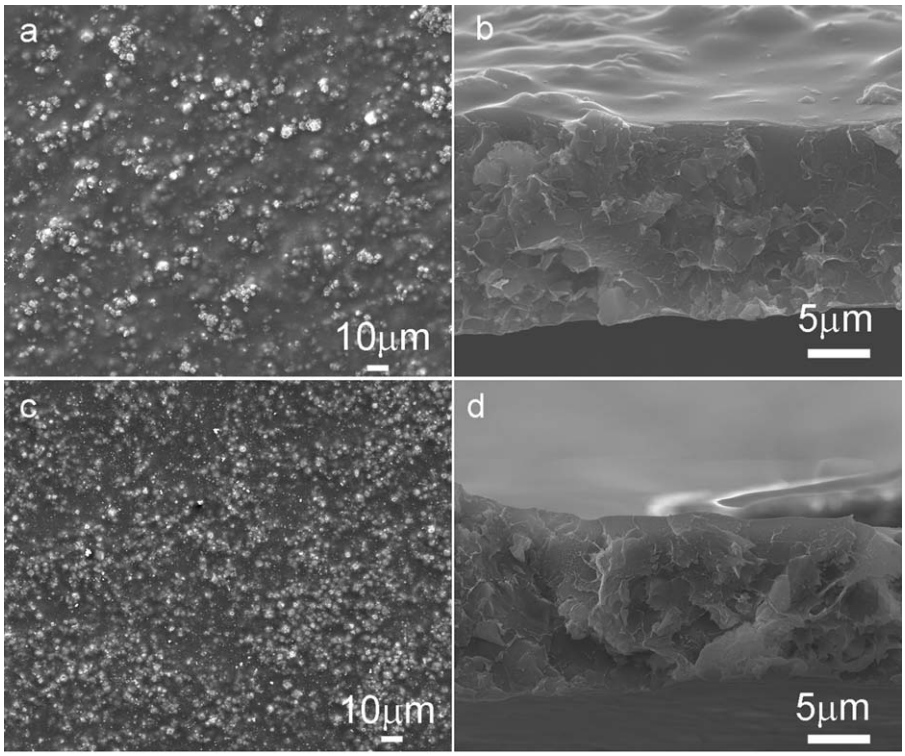

Figure 7. SEM images of 39.5 wt % ZIF-11/PBI composite membranes prepared with NMP (a and b) and DMAc (c and d) as the solvent. Surface (a and c) and cross-section (b and d) are shown.

top surfaces and cross-sections of 39.5 wt % ZIF-11/PBI composite membranes. The addition of ZIF-11 particles makes the membrane surface rough [Figure 7(a,c)] because of the presence of some ZIF-11 particles. The cross-sectional SEM images of ZIF-11/PBI composite membranes are shown in Figure 7(b,d). The thickness of the membrane is around 15 μm for both membranes. No boundary gaps or voids are observed in SEM images, which reveal a good PBI and ZIF-11 interaction. A uniform dispersion of ZIF-11 is obtained in both ZIF-11/PBI composite membranes, suggesting that the compatibility between ZIF-11 and PBI is very well.

Single-Gas Permeation of ZIF/PBI Composite Membranes

The single-gas permeability and ideal selectivity of H_2/CO_2 were measured at room temperature. For the pure PBI membrane prepared using DMAc as the solvent, the permeabilities of H_2 and CO_2 are 17.2 and 3.4 Barrer, respectively, with H_2/CO_2 ideal selectivity of 5.0. It is noted in the literature that the pure PBI membrane had a H_2/CO_2 selectivity of 8.6 with the hydrogen permeability of 3.7 Barrer.[8,15] The permeability is only one-fourth of our result. This may arise from the different raw materials used for membrane fabrication. The PBI solution contains 1.5 wt % of LiCl, and the removal of LiCl may introduce small defects in membrane, making the membrane have a low H_2 separation performance, but high permeability. With the incorporation of ZIF-11 from 16.1 to 39.5 wt %, the permeabilities of H_2 and CO_2 significantly increase. For the 16.1 wt % ZIF-11/PBI membrane, the H_2/CO_2 ideal selectivity is 5.6; it is slightly below the Robeson upper bound.[3] By further increasing the ZIF-11 loadings to 29.7 and 39.5 wt %, the ideal selectivity of H_2/CO_2 decreases to 3.7 and 3.6, respectively, which is probably due to the fact that (1) the particle size of ZIF-11 is too large (0.5–4.5 μm) that leads to a large free volume of PBI polymer, and (2) too many ZIF-11 in PBI polymer will form a shortcut for gas separation and may induce more defects.[8] For pure PBI membrane prepared in NMP solvent, the ideal selectivity of H_2/CO_2 is 3.4 with H_2 and CO_2 permeabilities of 16.5 and 4.8 Barrer, respectively. The low ideal selectivity possibly arises from the effect of the mixed solvents of DMAc (as-received PBI was kept in DMAc) and NMP. However, when 16.1 wt % of ZIF-11 was incorporated into PBI membrane, the permeabilities of H_2 and CO_2 were twice higher than those of pure PBI

Table I. Single-Gas Separation Performance of Pure PBI Membranes and ZIF-11/PBI Composite Membranes Prepared with DMAc and NMP as Solvent

		Permeability (Barrer)		
Sample	Solvent	H_2	CO_2	Selectivity (H_2/CO_2)
Pure PBI	DMAc	17.2	3.4	5.0
16.1 wt % ZIF-11-PBI	DMAc	67.8	12.1	5.6
29.7 wt % ZIF-11-PBI	DMAc	133.1	36.3	3.7
39.5 wt % ZIF-11-PBI	DMAc	464.7	128.2	3.6
Pure PBI	NMP	16.5	4.8	3.4
16.1 wt % ZIF-11-PBI	NMP	32.7	9.6	3.4

(Table I), indicating that ZIF-11 particles indeed increase the gas permeabilities. As the micrometer-sized ZIF-11 crystals are not optimal for the fabrication of polymer MMMs,[4] further work will be undertaken to prepare nanosized ZIF-11 for this purpose.

CONCLUSIONS

ZIF-11 crystals were successfully incorporated into PBI membrane for hydrogen separation. PBI is the suitable polymer for ZIF-11 incorporation when compared with PS and PES because ZIF-11 has a good compatibility with PBI matrix as they have the same benzimidazole structure. The incorporation of ZIF-11 increases the gas permeabilities of both H_2 and CO_2. The 16.1 wt % ZIF-11/PBI composite membrane prepared using solvent DMAc showed a slightly increased H_2/CO_2 ideal selectivity of 5.6 and about four times higher permeabilities than those of pure PBI. ZIF-11/PBI composite membrane has potential for hydrogen separation, and ZIF-11 can be extended to prepare in other polymer matrix for gas separations.

ACKNOWLEDGMENTS

This work is supported by the Australian Research Council and the Monash University. H. Wang thanks the Australian Research Council for a Future Fellowship. J. Yao thanks the support of Monash University through the Monash Fellowship Scheme.

REFERENCES

1. Baker, R. W. *Ind. Eng. Chem. Res.* **2002**, *41*, 1393.
2. Wijmans, J. G.; Baker, R. W. *J. Membr. Sci.* **1995**, *107*, 1.
3. Robeson, L. M. *J. Membr. Sci.* **2008**, *320*, 390.
4. Yao, J. F.; Wang, H. T. *Chem. Soc. Rev.* **2014**, *43*, 4470.
5. Noble, R. D. *J. Membr. Sci.* **2011**, *378*, 393.
6. Zimmerman, C. M.; Singh, A.; Koros, W. J. *J. Membr. Sci.* **1997**, *137*, 145.
7. Zhang, C.; Zhang, K.; Xu, L.; Labreche, Y.; Kraftschik, B.; Koros, W. J. *AIChE J.* **2014**, *60*, 2625.
8. Yang, T. X.; Shi, G. M.; Chung, T. S. *Adv. Energy Mater.* **2012**, *2*, 1358.
9. Park, K. S.; Ni, Z.; Cote, A. P.; Choi, J. Y.; Huang, R.; Uribe-Romo, F. J.; Chae, H. K.; O'Keeffe, M.; Yaghi, O. M. *Proc. Natl. Acad. Sci. USA* **2006**, *103*, 10186.
10. Phan, A.; Doonan, C. J.; Uribe-Romo, F. J.; Knobler, C. B.; O'Keeffe, M.; Yaghi, O. M. *Acc. Chem. Res.* **2010**, *43*, 58.
11. Li, L. X.; Yao, J. F.; Chen, R. Z.; He, L.; Wang, K.; Wang, H. T. *Microporous Mesoporous Mater.* **2013**, *168*, 15.
12. Yao, J. F.; Dong, D. H.; Li, D.; He, L.; Xu, G. S.; Wang, H. T. *Chem. Commun.* **2011**, *47*, 2559.
13. Chung, T. S.; Xu, Z. L. *J. Membr. Sci.* **1998**, *147*, 35.
14. Choi, S. H.; Coronas, J.; Lai, Z. P.; Yust, D.; Onorato, F.; Tsapatsis, M. *J. Membr. Sci.* **2008**, *316*, 145.
15. Yang, T. X.; Xiao, Y. C.; Chung, T. S. *Energy Environ. Sci.* **2011**, *4*, 4171.
16. Yang, T. X.; Chung, T. S. *J. Mater. Chem. A* **2013**, *1*, 6081.
17. Yang, T. X.; Chung, T. S. *Int. J. Hydrogen Energy* **2013**, *38*, 229.
18. Thornton, A. W.; Dubbeldam, D.; Liu, M. S.; Ladewig, B. P.; Hill, A. J.; Hill, M. R. *Energy Environ. Sci.* **2012**, *5*, 7637.
19. He, M.; Yao, J. F.; Liu, Q.; Zhong, Z. X.; Wang, H. T. *Dalton Trans.* **2013**, *42*, 16608.
20. Chang, Z. H.; Pu, H. T.; Wan, D. C.; Liu, L.; Yuan, J. J.; Yang, Z. L. *Polym. Degrad. Stab.* **2009**, *94*, 1206.